

FINAL REPORT ON MAGLEV SYSTEM

AUTOMATION AND CONTROL LABORATORY

[ALESSANDRO FALSONE]



POLITECNICO

MILANO 1863

AUTOMATEAM

Members: Francesco Ferraboli, Yevhen Ihnatov, Enrico Falco, Elaheh Hajitalebi

June 2023

Abstract

The Magnetic Levitation plant comprised of electromagnetic subsystems with the functionality of levitating a steel ball in an air gap of 14mm has been analyzed in detail.

A non-linear mathematical model is developed starting from data sheets of the producer and physics theory. The physical parameters of the system are identified to complete the model, required controllers are designed and implemented, then the performance of the closed loop system is validated and coherence of the results with that of the desired performance are compared.

The electrical circuit requires a current controller which is used to control the excitation of the nonlinear subsystem for ball positioning model; thanks to the current sensor the PI current controller is designed and implemented.

To achieve the aim of the project, it is needed to lift the ball and keep it firmly in the desired position and track the reference, hence the position controller is designed. Taking advantage of root locus, pole placement and LQG, controllers are designed in both frequency and state space domain. Also, the advanced position controller is considered and designed with different techniques such as: backstepping, variable structure (sliding surface) and feedback linearization. Ultimately the one with feedback linearization is developed and implemented perfectly.

Due to the intense nonlinear and unstable behavior of the system and the low efficiency of photo sensitive voltage-position sensor, obtaining the desired and qualified performance was a great challenge that finally with detailed considerations we coped with and the purposes of the project are fulfilled.

Contents

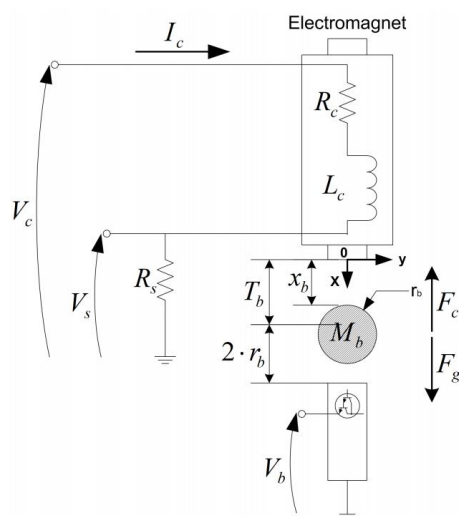
1. System Modeling	4
1.1. Electrical subsystem.....	5
1.2. Nonlinear subsystem	5
1.2.1. Nonlinear steady state representation of the subsystem	6
1.2.2. Further consideration on the model	8
2. Parameter identification	9
2.1. Electrical subsystem parameters identification	9
2.1.1. R Identification	9
2.1.2. τ Identification	9
2.1.2.1. τ identification through observation of the step response:	9
2.1.2.2. τ identification through Least Square Method	10
2.1.3. L Identification.....	10
2.2. Nonlinear subsystem parameters identification	10
2.2.1. K identification through Lift up in open loop:.....	11
2.2.2. K identification in closed loop:.....	11
2.2.3. Mapping function between read voltage and position in meters	11
3. Validation of the model in open loop	12
3.1. Validation of Electrical subsystem in open loop.....	12
3.2. Validation of nonlinear subsystem in open loop:.....	13
4. Control design	15
4.1. Current controller for the electrical subsystem	15
4.1.1. Validation of electrical subsystem model in closed loop with Current controller.....	16
4.2. Position controller for the nonlinear subsystem	18
4.2.1. Root Locus position controller.....	18
4.2.1.1. Validation of nonlinear subsystem model in closed loop with Root Locus controller ..	20
4.2.2. Pole placement position controller in cascade	22
4.2.2.1. Validation of closed loop system with Pole placement position controller in cascade.	24
4.2.3. LQG position controller in cascade	27
4.2.3.1. Validation of closed loop system with LQG controller in cascade	29
4.2.4. Feedback linearization controller (Advanced).....	32
4.2.4.1. Validation of closed loop system with feedback linearization position controller	34

1. System Modeling

The first step in the project is to investigate the structure of the system to obtain a precise model which corresponds with the actual plant.

The MAGLEV plant is an electromagnetic suspension system acting on a solid one-inch steel ball. It mainly consists of an electromagnet, located at the upper part of the apparatus, capable of lifting from its pedestal and sustaining in free space the steel ball. Two system variables are directly measured which are the coil current and the ball distance from the electromagnet face. Mechanical and electrical specifications of the system are listed below:

Symbol	Description	Value	Unit
c_{max}	Maximum Continuous Coil Current	3.0	\pm A
L_c	Coil Inductance	412.5	mH
R_c	Coil Resistance	10	Ω
N_c	Number Of Turns in the Coil Wire	2450	
l_c	Coil Length	0.0825	m
r_c	Coil Steel Core Radius	0.008	m
K_m	Electromagnet Force Constant	6.5308×10^{-5}	$N - m^2 / A^2$
R_s	Current Sense Resistance	1	Ω
r_b	Steel Ball Radius	1.27×10^{-2}	m
M_b	Steel Ball Mass	0.068	kg
T_b	Steel Ball Travel	0.014	m
g	Gravitational Constant on Earth	9.81	m/s^2
μ_o	Magnetic Permeability Constant	$4\pi \times 10^{-7}$	H/m
K_B	Ball Position Sensor Sensitivity (Assuming a User-Calibrated Sensor Measurement Range from 0 to 5 V)	2.83×10^{-3}	m/V



Proceeding with modelling, each subsystem of the overall setup is considered individually and by examining the system with different experiments, parameters and finally an accurate model is obtained. The Maglev setup contains an electrical subsystem and a magnetic subsystem which respectively the procedure is developed below:

1.1. Electrical subsystem

The internal electrical circuit comprised of the resistor (R) and an inductor (L) of the coil in series should be modeled, so simply a first order model of an RL circuit is acquired dismissing the temperature effect and the negligible resistance of the current sensor through the following equations by Kirchhoff's voltage law being (V) applied coil voltage and (i) coil current:

$$V = Ri + L \frac{di}{dt}$$

This can be represented by the first-order transfer function:

$$\frac{I}{V} = \frac{1}{R + LS} \quad \frac{I}{V} = \frac{1/R}{1 + L/R S}$$

$$\langle G(s) = \frac{1}{V} = \frac{1/R}{1 + \tau S} \rangle$$

Being $1/R$ the DC gain, and τ constant time. R, L and τ are parameters of the system which should be identified and validated in order to become certain that the modeled system is trustable enough.

1.2. Nonlinear subsystem

In this case due to the nonlinearity of the attraction force generated by the electromagnet, it is supposed to start dealing with a nonlinear system. Being D the airgap distance between the ball and the face of the electromagnet, air friction is neglected and the ball in space has 6 degrees of freedom but here we consider just the vertical translation which is the one we are able to control with this setup.

$$L = \frac{N^2 A \mu}{D} \quad N \text{ number of the turns in the coil, } A \text{ area involved in magnetic field, } \mu \text{ magnetic permeability constant}$$

$$F = \frac{d}{dD} \left(\frac{1}{2} L i^2 \right) \quad F \text{ Force generated by electromagnet through the derivative of the magnetic energy with respect to } D$$

$$F = \frac{N^2 A \mu}{2} \frac{i^2}{D^2} \quad \text{The pull of the electromagnet is proportional to the square of the current and inversely proportional to the air gap squared}$$

Owing to the fact that computation of the area involved in the magnetic field is complex to be obtained and in addition being provided with the electromagnet force constant (K_m) in the specification table given by the manufacturer the decision is to include area in K_m and in the further steps identify the electromagnet force constant.

$$F = K_m \frac{i^2}{2 D^2}$$

To simplify the equation and get rid of the extra constant values, we encapsulate all and introduce a new parameter K which is needed to be identified and validated in section 2.2.1.

$$F = K \frac{i^2}{D^2}$$

The force due to gravity acting on the ball is given by $F_g = Mg$

Regarding the mass of the ball, M , we trusted the data sheets without further investigations and tests.

Applying then Newton's second law of motion to the ball gives the following nonlinear Equation of Motion:

$$\begin{cases} \sum F = M a \\ Mg - K \frac{i^2}{D^2} = M \ddot{D} \end{cases} \xrightarrow[\begin{smallmatrix} \dot{D} = 0 \\ \ddot{D} = 0 \end{smallmatrix}]{\text{Equilibrium}} \begin{cases} D_{eq} = \sqrt{\frac{K}{Mg}} \quad l_{eq} \\ K = \frac{M g D^2}{I^2} \end{cases}$$

Therefore, the amount of the ball distance and electromagnetic force constant in the equilibrium would be computed through the last two formulas above.

1.2.1. Nonlinear steady state representation of the subsystem and linearization

$$\begin{cases} x_1 = D \\ x_1' = x_2 = \dot{D} \\ x_2' = \ddot{D} = g - \frac{K}{M} \frac{i^2}{x_1^2} \end{cases}$$

In the equation above two states are defined: the distance of the ball from the magnet D and \dot{D} , which is the velocity of the ball. One of the challenges in this project is the fact that the velocity of the ball is not a measurable parameter, so it will be estimated through different techniques. Furthermore, the optical sensor is intensively sensitive to brightness's variations, which is a further source of uncertainty. Trying to cope with this issue we covered the setup to have darkness. We noticed it was more reliable in the sense that we didn't need to change it over time anymore.

Being our model nonlinear, in order to be able to have a decent model of the system and then design a linear controller, we proceed with linearization around the static equilibrium point, where the ball is suspended in a constant position.

To design a frequency-based controller capable to keep the ball in position, we have linearized the system around an equilibrium point D_{eq} as follows:

$$\begin{cases} x_1' = x_2 \\ x_2' = g - \frac{K}{M} \frac{i^2}{x_1^2} = f_2 \end{cases}$$

Looking at second equation of the model it is clear that only an attractive force can be applied (current is squared) and that is the reason we made sure never a negative current is applied on the system through saturations.

In the case of the levitated ball, the operating range corresponds to small departure positions, δx_1 , from the desired equilibrium point \bar{x}_1 . Therefore: $\delta x_1 = x_1 - \bar{x}_1$

$$\begin{cases} \delta \dot{x}_1 = \delta x_2 \\ \delta \dot{x}_2 = \frac{\delta f_2}{\delta x_1} \delta x_1 + \frac{\delta f_2}{\delta i} \delta i = \frac{2K\bar{i}^2}{M\bar{x}_1^3} \delta x_1 - \frac{2K\bar{i}}{M\bar{x}_1^2} \delta i \end{cases}$$

At this point the equation of the motion is linearized and by the definition we have $\delta x = Ax + Bu$, so by substituting the values of the parameters in the equilibrium (in the section 1.2.) and through the identification of K (in the section 2.2.1), one can obtain the initial linear representation of the system.

$$A = \begin{bmatrix} 0 & 1 \\ \frac{2K\bar{i}^2}{M\bar{x}_1^3} & 0 \end{bmatrix} \quad B = \begin{bmatrix} 0 \\ -\frac{2K\bar{i}}{M\bar{x}_1^2} \end{bmatrix}$$

$$\begin{cases} D_{eq} = \sqrt{\frac{K}{Mg}} I_{eq} \longrightarrow D_{eq} = \bar{x}_1 = 0.007 \\ K = \frac{Mg D^2}{l^2} \longrightarrow \bar{i} = \sqrt{\frac{Mg}{K} \bar{x}_1} = 0.976 A \end{cases}$$

The value of parameters in the equilibrium are computed, hence one obtains the initial linear matrices corresponding to the linearized system around the equilibrium.

$$A = \begin{bmatrix} 0 & 1 \\ 2801.69 & 0 \end{bmatrix} \quad B = \begin{bmatrix} 0 \\ -20.09 \end{bmatrix}$$

But it should be considered that the final transfer function is not the one corresponded to these two matrices, in order to have a precise model, initially the model corresponded to these matrices is obtained and the initial controller is designed with the only purpose of keeping the ball in the equilibrium point which is $D_{eq} = \bar{x}_1 = 0.007$, then the measured current value at this point is read through the current sensor which is $\bar{i} = 1.05$. At this point with all these considerations and substituting the new and precise values, one can obtain a final model which is reliable enough.

$$A = \begin{bmatrix} 0 & 1 \\ 2802.9 & 0 \end{bmatrix} \quad B = \begin{bmatrix} 0 \\ -18.69 \end{bmatrix}$$

Although, there is not a remarkable difference between the results of these two approaches, the last parameters which are yielded by the sensor measurement are more reliable and for the further steps, these values are considered.

Finally having matrices, A and B, the transfer function associated to linearized system is obtained:

$$\langle G_d(s) = \frac{X}{I} = \frac{-18.69}{s^2 - 2803} \rangle$$

The linearized system shows two real poles: one positive and one negative.

1.2.2. Further consideration on the model

Up to now we have considered a model which is continuous time, and the design of our controller will be made with the same assumption. However, the real system is made of an elaboration system in discrete time, so it's required to keep into account also the presence of a A/D converter, a D/A converter and the elaboration time. All these components can be summarized through a simple time delay transfer function, known as discretization delay which is: $e^{-s\frac{T}{2}}$ where $T = \frac{2\pi}{\omega_s}$ and ω_s is the validation and control design frequency. Also the sampling induced delay is considered: $e^{-s\frac{T_s}{2}}$

2. Parameter identification

Here is presented the identification of the parameters, which are required to complete our model. They will be found performing different experiments, in particular the electrical parameter identification will be carried out applying a constant voltage and a step. The parameter K will be identified through a lift up experiment.

2.1. Electrical subsystem parameters identification

The achieved model in the section 1.1. associated to the electrical internal circuit is:

$$\langle G(s) = \frac{1}{V} = \frac{1/R}{1 + \tau s} \rangle$$

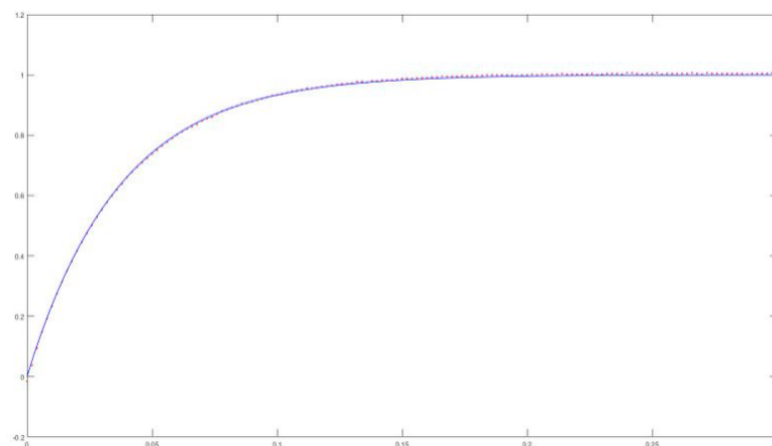
The parameters to be identified are the resistance R and the time constant τ (through which is possible to find the inductance L).

2.1.1. R Identification: The approach to identify this parameter is taking advantage of the steady state gain. The procedure is to apply a constant voltage to the system and read the measured current. So, applying a dc voltage in the range (V) of 10V we read a value of current $I \cong 1A$ is stored. Since, at steady state there is no voltage drop on the inductance, R is obtained as:

$$R = \frac{V}{I} \cong \frac{10}{1} \cong 10 \Omega$$

2.1.2. τ Identification: The approach to identify this parameter is taking advantage of Least square Method combined with observation. τ is identified by observing the step response and in addition, through least square by the minimization of a cost function.

2.1.2.1. τ identification through observation of the step response:



Given a step, the time constant τ is the time required to reach 0.63 of its final value. In our case, observing the step response, we have seen that approximately $\tau = 0.04$.

2.1.2.2. τ identification through Least Square Method

In order to reach a more precise identification of the time constant τ , we decided to apply the optimization technique known as least square method. The procedure consists in find the τ which minimizes the distance between an ideal exponential decay function and our current output. The computation has been made using excel as shown below:

$$\tau = \operatorname{argmin} \sum (i(1 - e^{-t/\tau}) - I)^2$$

	A	B	C	D	E	F	G	H	I
1	0	0,002	0,004	0,006	0,008	0,01	0,012	0,014	0,016
2	-0,019226661	-0,01923	-0,02167	-0,01923	-0,01923	-0,01923	-0,01679	-0,01923	-0,01923
3	-0,01678518	0,036927	0,093081	0,146794	0,190741	0,232246	0,273751	0,312815	0,34923
4	-0,01678518	0,036927	0,093081	0,146794	0,190741	0,232246	0,273751	0,312815	0,34923
5	tau								
6	0,037194885								

Finally, τ is identified approximately $\tau \cong 0.037s$

2.1.3. L Identification: By definition, inductance is the production of time constant and resistance, simply identifying the parameters τ and R , L would be identified:

$$L = \tau \times R \cong 0.37 H$$

In summary, the identified model of electrical subsystems is:

$$\langle G(s) = \frac{I}{V} = \frac{1/R}{1 + \tau s} = \frac{0.1}{0.037s + 1} \rangle$$

2.2. Nonlinear subsystem parameters identification

The achieved linearized model in the section 1.2.1. associated to the nonlinear subsystem expressed in state space is:

$$A = \begin{bmatrix} 0 & 1 \\ \frac{2K\bar{t}^2}{M\bar{x}_1^3} & 0 \end{bmatrix} \quad B = \begin{bmatrix} 0 \\ -\frac{2K\bar{t}}{M\bar{x}_1^2} \end{bmatrix}$$

Where K (the electromagnet force constant) is the parameter, we have to identify. Since the system is unstable it's not possible (in open loop) to stay in an equilibrium position, so the only possible approach for the identification of k is through a lift up experiment, where we consider as equilibrium current the values we have read just before the starting of the lift up. Once the controller has been designed, we have performed another experiment in closed-loop in an actual equilibrium position in order to identify a more meaningful parameter value.

2.2.1. K identification through Lift up in open loop:

We decided to apply a slow ramp of voltage in order to lift up the ball, measuring the excitation current with the sensor when the ball is in the threshold to lift up. The result is $I \cong 1.9 \text{ A}$. Knowing that the ball was initially in position $D = 14 \text{ mm}$, K is given by the following equation:

$$K = \frac{M g D^2}{I^2} \cong 3.43 \times 10^{-5}$$

2.2.2. K identification in closed loop:

Through the controller designed starting from the K identified in open-loop, we have later performed another experiment, this time in closed-loop, while the ball was stable around the equilibrium point. The value we've found is here reported:

$$K_{mid} = \frac{M g D^2}{I^2} \cong 2.96 \times 10^{-5}$$

In summary, the identified transfer function of the linearized model of the nonlinear subsystem is:

$$\langle G_d(s) = \frac{X}{I} = \frac{-18.69}{s^2 - 2803} \rangle$$

2.2.3. Mapping function between read voltage and position in meters

The position sensor of the apparatus gives us as output a voltage, so a mapping function has been required in order to read the position in millimeters.

To do so, we have performed 2 experiments: one placing the ball on the pedestal and the second one attaching it to the top, reading the corresponding V_{min} and V_{max} . The mapping consists in a linear function which pass through these 2 points.

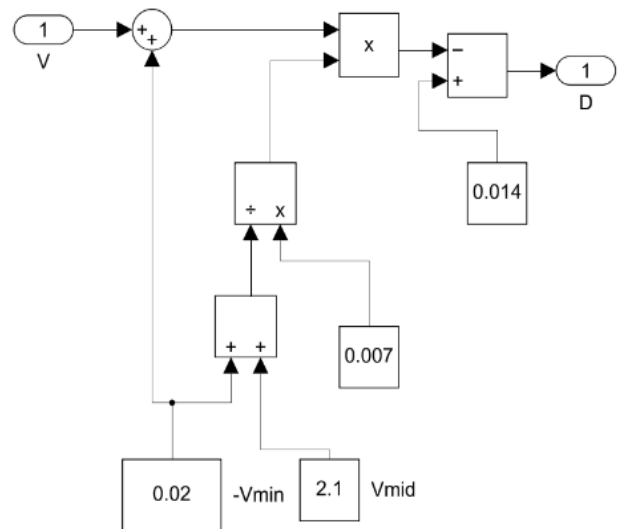
d : the distance from position sensor(bottom)

D : the distance from the top $D = 0.014 - d$

The initial mapping function is defined as:

$$d = \frac{0.014}{V_{max} - V_{min}} (V - V_{min})$$

We have later decided (since we consider the middle position our working point) to it, using V_{mid} instead of V_{max} , where V_{mid} has been found once we had a controller to keep the ball in position.



3. Validation of the model in open loop

Once the model of the system is obtained, it is required to validate the model and confirm its accuracy. The purpose is to apply the same signal to both the actual plant and the modeled one and verify the confirmation of their output. We expect the modeled system to manifest the same behavior as that of the actual plant while exposed to the same input in the same situation. In order to achieve this result, initially the validation of electrical subsystem model is analyzed both in frequency and time domain. Then, the validation of linearized subsystem related to the positioning is analyzed.

3.1. Validation of Electrical subsystem in open loop

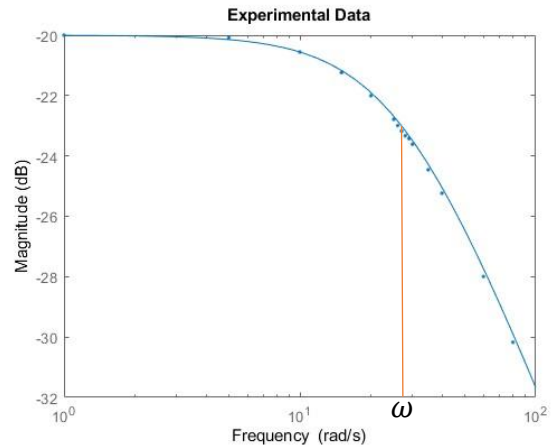
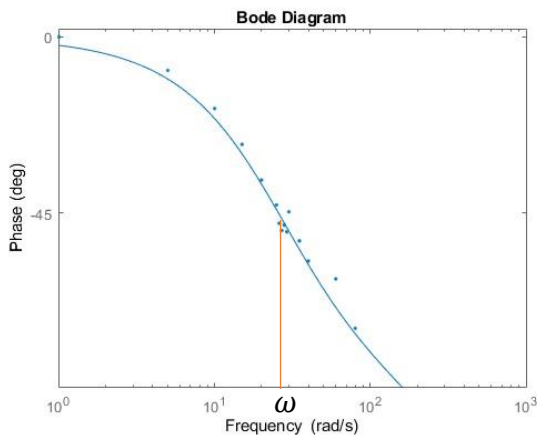
3.1.1. In frequency domain

Model:

$$\left\langle G(s) = \frac{I}{V} = \frac{1/R}{1 + \tau s} = \frac{0.1}{0.037s + 1} \right\rangle$$

Pole frequency: $\omega = 1/\tau = 1/0.037 \cong 27 \text{ rad/s}$

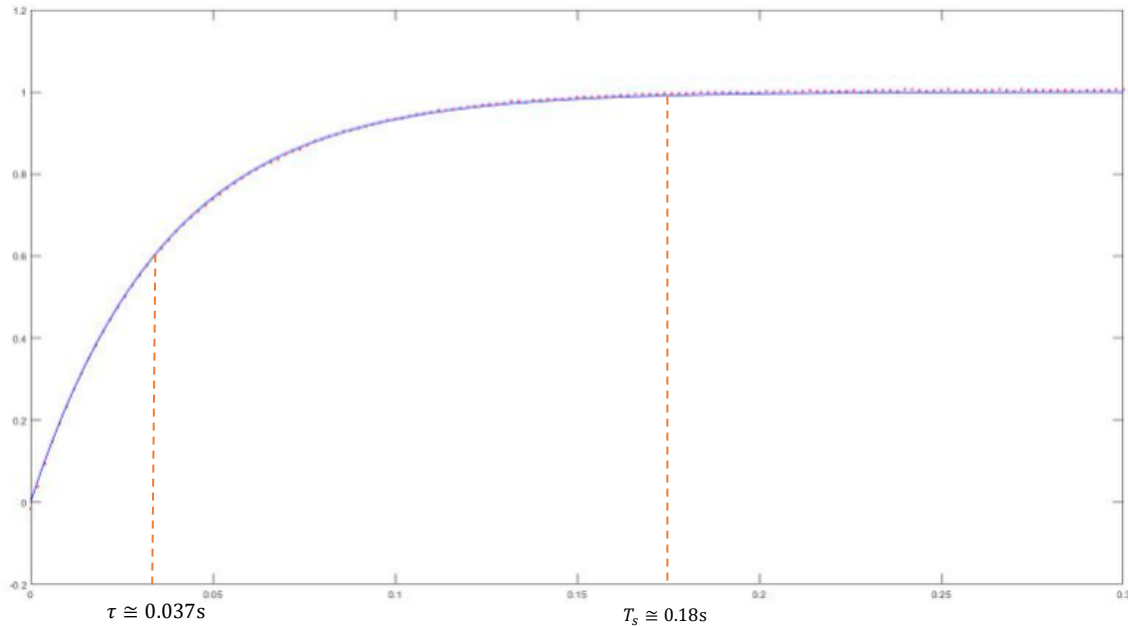
Method: Sinusoidal waves of different frequency (even beyond the pole frequency) with magnitude of 10 V are applied to the actual system and the bode diagrams of gain and phase are compared to the ones of our model transfer function:



Analysis: The electrical model in open loop successfully conforms the output of the actual plant for both phase and amplitude and the decrease of slope in bode diagram of the gain and decrease of the phase due to the pole around $\omega \cong 27 \text{ rad/s}$ and also the $gain = \frac{I}{V} = -20 \text{ dB} = 0.1$ is detectable. (Points being the gain of the subsystem corresponded to the frequency of applied sinusoidal wave, and the constant line being the gain of the model).

3.1.2. In time domain

In this case the method consists in apply a step to the actual system and the modeled one and validate whether the step responses of both are compatible. Hence, a step signal of 10 V is applied and the step response is depicted below:



Analyze: Being time constant 0.63 of final value, through the graph it is detectable that $\tau \approx 0.037\text{s}$, also settling time according to the definition $T_s = 5 \times \tau \approx 0.18$ is satisfied and they pretty much overlap. The response is good since we neither have overshoot nor oscillations.

3.2. Validation of nonlinear subsystem in open loop:

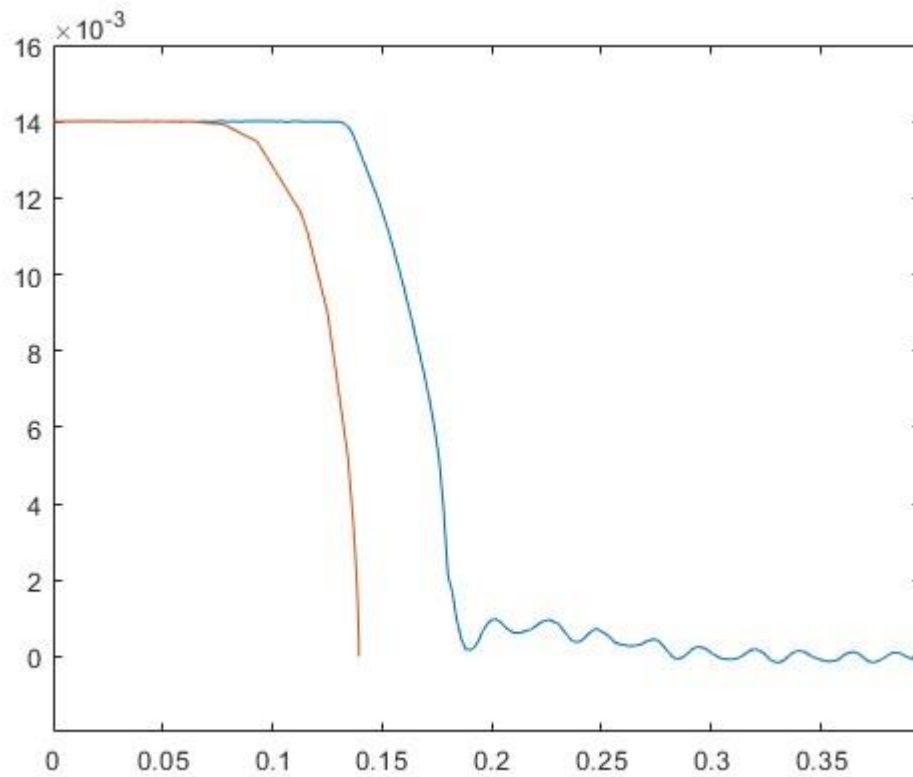
Model:

$$\langle G_d(s) = \frac{X}{I} = \frac{-18.69}{s^2 - 2803} \rangle$$

In this case due to the high oscillation of the ball being exposed to a high nonlinear dynamic, validation of the model is accomplished in time domain rather than in frequency domain.

We performed the test by applying a constant voltage of 23 V that we knew it was enough to lift up the ball and compared the position read by the sensor with the one seen through the scope in simulation. This is possible thanks to a non-linear model realized on Simulink which represents also the ball on the bottom through some logic. The simulation automatically stops when the ball reaches 0 mm of air gap (when it comes in contact with the magnet) because of singularity reasons: in the expression of the magnetic force, we have the position squared at the denominator. But this is a fine since when the ball reaches the top even if we apply zero voltage (which in turns gives zero current and so zero force).

In the figure are shown the position scope during the real lift-up (blue) and the simulated one (red):



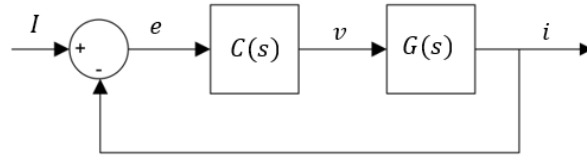
The two curves are quite similar even if the time at which the ball in simulation starts to move comes earlier than the real one. We have performed some experiments, seeing that adjusting our K the 2 curves match quite perfectly. We are not really surprised by this, since our K is the result of an experiment intrinsically uncertain and moreover K itself is just an approximation of the real behavior, that we have seen is a function that changes over time.

4. Control design

Accordingly with the aim of the project, the ball should be kept firmly in the middle of the air gap. To do so, the coil current which excites the magnet should be controlled to create the desired magnetic field which forces the ball to travel in the gap. Therefore, in the first step it is required to control the coil current. Then to fulfill the positioning of the ball, it is required to design a ball position controller, in this project 4 types of ball positioning controllers are designed and implemented which would be explained in the section 4.2.

4.1. Current controller for the electrical subsystem

Given the plant model $G(s) = \frac{0.1}{0.037s+1}$ a coil current controller is designed in order to fulfill the objectives of the project. As a specification for this aim a response time of $T_r = 0.02 \text{ s}$ is desired. So, a controller is designed such that the closed loop subsystem reaches this response time.



Because of limitations of the actuator and safety measurements not to damage the setup, saturation on both the voltage and current are introduced. Considering the simple first order model, a PI controller is designed through zero-pole cancellation and to avoid wind-up phenomena an anti-windup scheme has been implemented.

PI controller:

$$C(s) = 2500 \frac{0.037s + 1}{s}$$

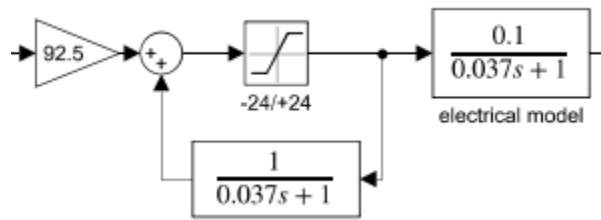
Open loop transfer function:

$$Go(s) = C(s) \times G(s) = 2500 \frac{0.037s + 1}{s} \times \frac{0.1}{0.037s + 1} = \frac{250}{s}$$

Closed loop transfer function:

$$Gc(s) = \frac{Go}{1 + Go} = \frac{1}{1 + 0.004s}$$

Therefore, $\tau = 0.004 \text{ s}$, $T_r = 5 \times \tau = 0.02 \text{ s}$ with this controller the desired specifications of the system are satisfied. The overall controller considering the anti-windup effect:



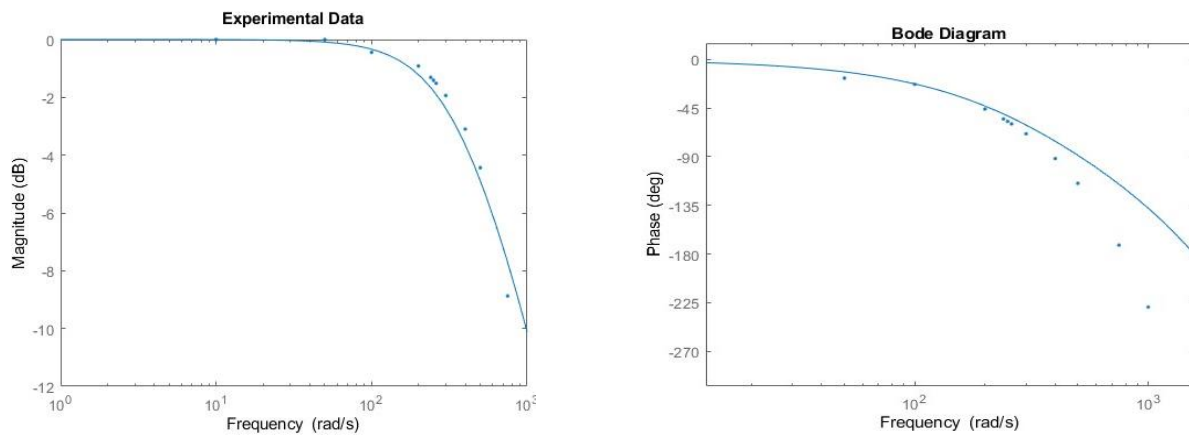
The voltage saturation (+24 V/-24 V) is provided with the datasheet, but we noticed the system cannot go over approximately 2.2 A so we later on lowered the saturation to (+22 V/-22 V). This controller has an ideal phase margin of 90° but it goes down to 75,7° taking in consideration the delay caused by the sample time of 2 ms.

4.1.1. Validation of electrical subsystem model in closed loop with Current controller

Validation is carried on both in frequency and time domain, The procedure is explained before with the difference that in this case the system is closed loop and the overall performance of electrical subsystem with current controller is analyzed. All the considerations and graphs here presented include the time delay discussed in section 1.2.2.

In frequency domain

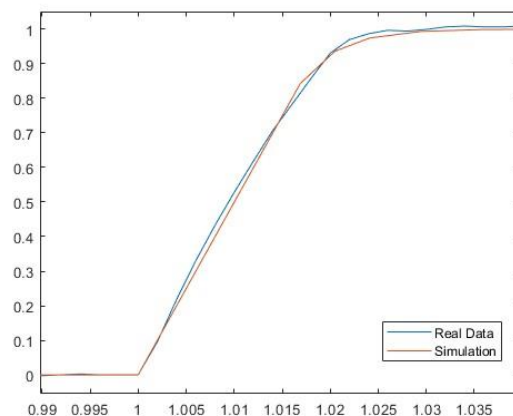
Here are presented the bode diagrams of the gain and the phase of both the real and simulated closed-loop systems where $F(s) = \frac{L(s)}{1+L(s)}$ with $L = Ci + Gel$



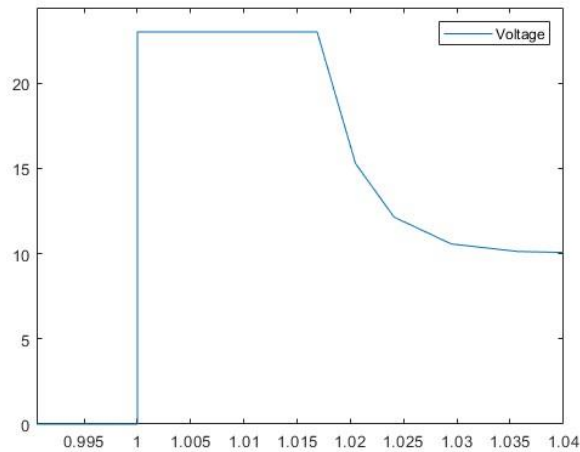
As can be seen, the gains are quite similar while there is some difference in terms of phase. It is supposed to be due to some further time delay we are not considering.

In time domain

Here are reported the two graphs that represent the step response of the real and simulated closed-loop system.

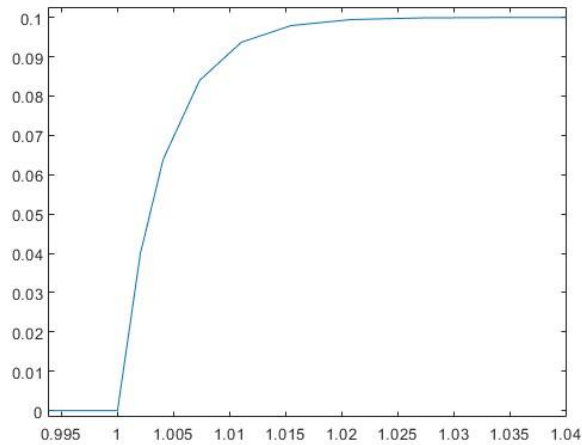


Analysis: Since $\omega = 250$ we should have $\tau = 1/250 = 0.004$ and a settling time of $5\tau = 0.02$; instead we have $T_s=0.025$ which gives us a $\tau = T_s/5 = 0.005$, that's because we have some saturation on the voltage which slows down the controller because it opens the loop. In fact, we can see how initially there isn't an exponential growth instead there is a linear one.



Initial voltage saturation seen during the step response

If instead we simulate a little step of just 0.1 A request, we recover the designed time response because saturation of the voltage isn't reached.



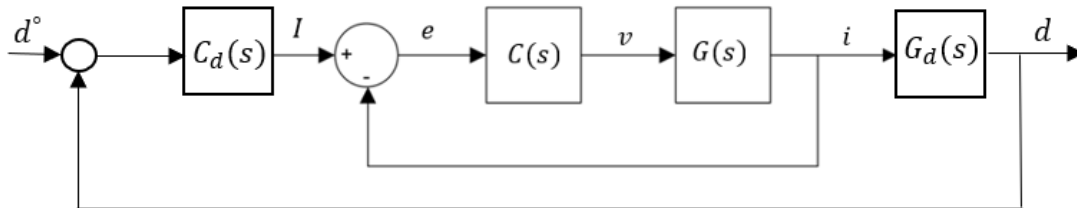
Step response without voltage saturation

Voltage saturation will be a problem when high steps of current are required like in lift-up.

4.2. Position controller for the nonlinear subsystem

Generally speaking, the overall system is a combination of an inner loop and an outer loop. Considering the inner system is the electrical one with the input voltage and the output current, and the outer system with the current input and position output. The decision is to design a position controller for the system which sends current as the reference set-point to the inner loop.

The structure of the system in cascade would be as below:



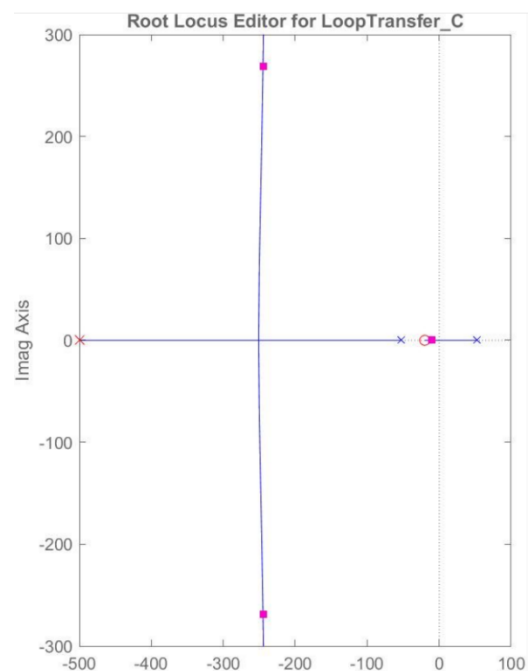
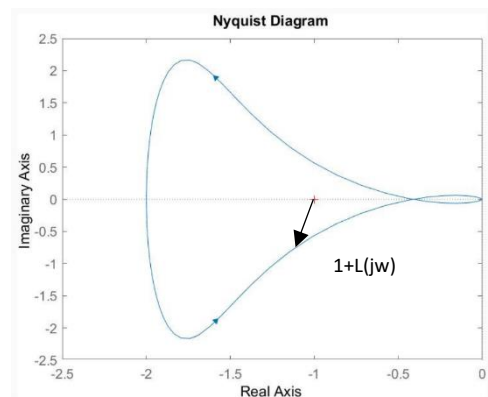
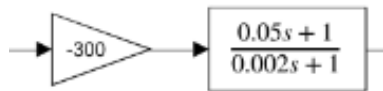
The position controllers in this project are designed through 4 different technics which will be described each in the related sections. The technics used for position controller are: Root locus, Pole placement, LQG and advanced feedback linearization.

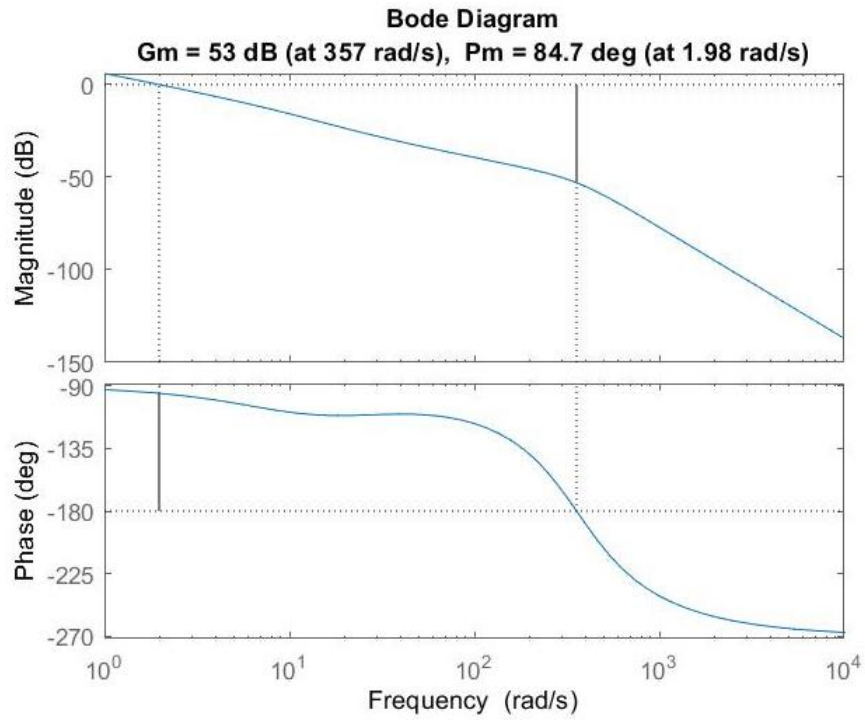
4.2.1. Root Locus position controller

Given the plant model $G_d(s) = \frac{x}{I} = \frac{-18.69}{s^2 - 2803}$ a position controller is designed to fulfill the objectives of the project. As a specification for this aim a response time of at least $T_r = 0.2$ s (which is 10 times slower than the one of the inner loop) is desired. So, a controller is designed such that the closed loop subsystem reaches this response time. In order to increase the robustness of the controller the Nyquist diagram (here plotted considering also delay) is analyzed to keep as much distance as possible from -1 (decreasing gain margin and increasing phase margin as much as possible) and avoiding instability. The Nyquist diagram needs to turn around -1 one time as the numbers of unstable poles. There is also an outer loop with an integrator for zero steady state error.

Root locus position controller:

$$C_d(s) = -300 \frac{0.05s + 1}{0.002s + 1}$$



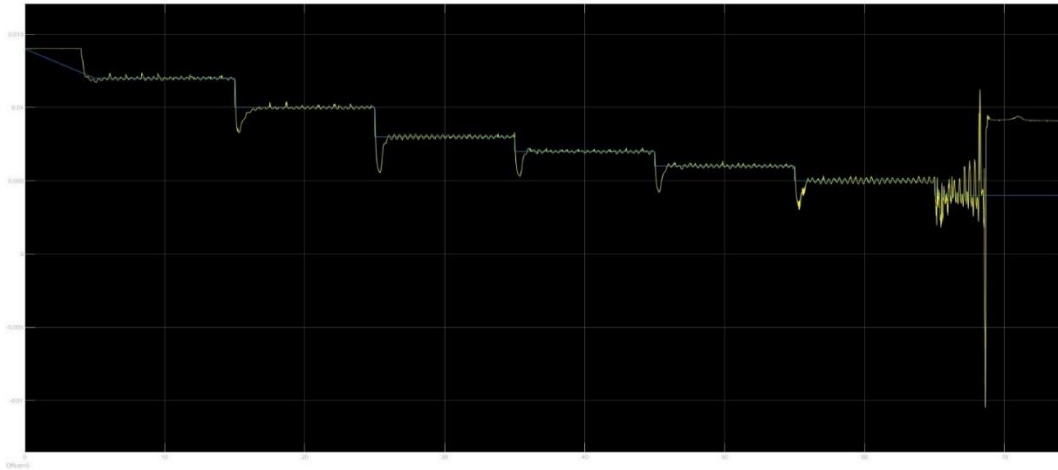


Overall open loop transfer function from reference to position

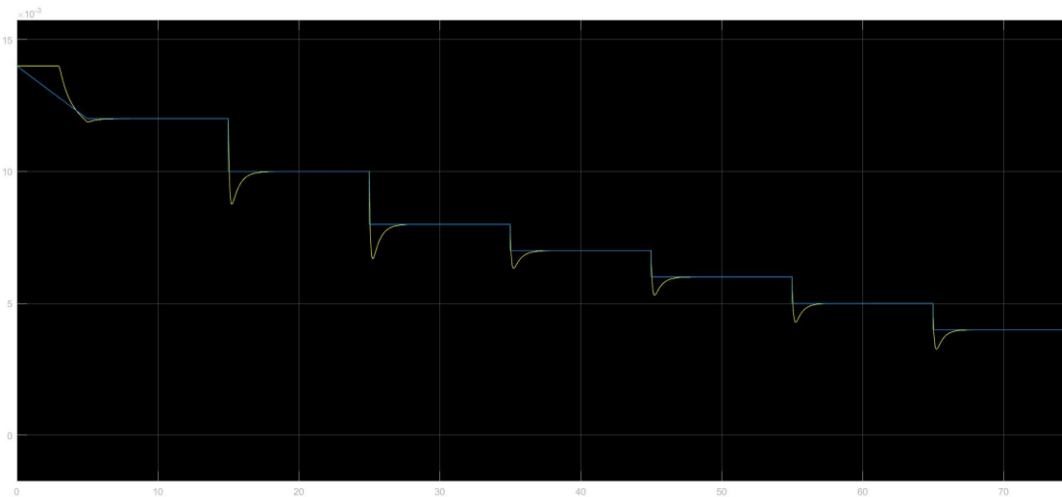
If we consider the vector that goes from -1 to the closest point on the Nyquist diagram of $L_{rl}(j\omega)$ it is defined $\min |1 + L_{rl}(j\omega)| = M_s^{-1}$ and can be proven that $\varphi_m \geq 2 * \arcsine\left(\frac{1}{2 * M_s}\right) = 44.26^\circ$

4.2.1.1. Validation of nonlinear subsystem model in closed loop with Root Locus controller

The following images represent the ball tracking (real and simulated) of a changing reference:



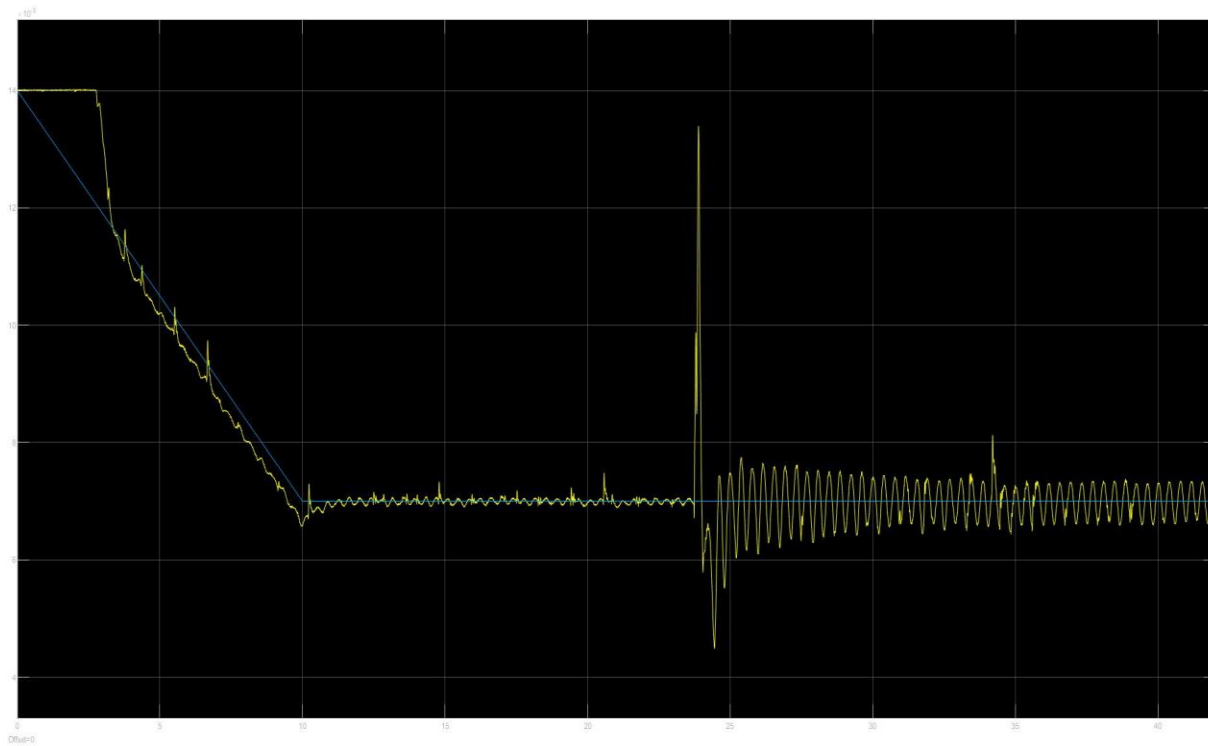
Position tracking of the real system



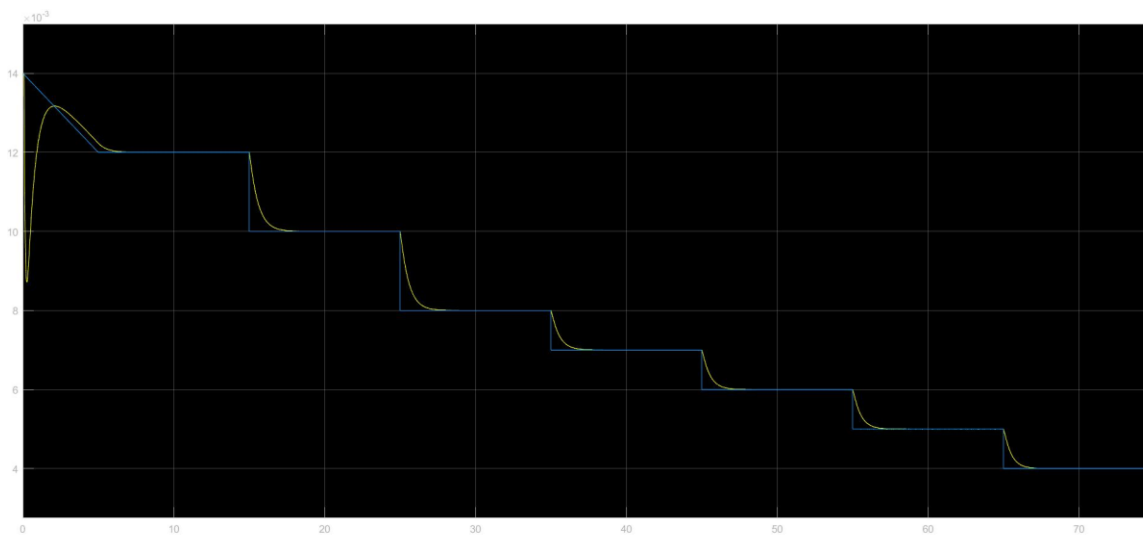
Position tracking in simulation

The reference consists of a ramp from 14 to 12 mm. Then increasing steps are applied: 10 mm, 8 mm, 7 mm, 6 mm, 5 mm and finally 4 mm, at which control is lost. This is a recurrent problem: the closer the ball approaches the magnet, the more difficult to be controlled. We were not expecting to see such a high overshoot, but we have understood later that this phenomenon was caused by an accidental mistake: instead of change directly the reference for the tracking we were keeping it at 0, modifying instead the equilibrium bias. Later will be shown the result in simulation changing the reference directly. In any case

the controller is quite robust with respect to disturbances as it is shown in the next figure in which the ball is lifted via a ramp to 7 mm and then a very strong impulsive force has been applied on the table where the setup was located. The control was able to retrieve the system stability even though not with the same amplitude of oscillation, this is caused by the fact that the disturbance introduces some further oscillations to the ball that MAGLEV 's hardware characteristics is incapable of mitigating.



Disturbance rejection experiment



Simulation tracking applying changes directly to the reference

4.2.2. Pole placement position controller in cascade

Pole placement is a method employed in feedback control system theory to place the closed loop of a plant in pre-determined locations in the s-plane. To design pole placement controller the same linearized model but in a different equilibrium point is used.

$$A = \begin{bmatrix} 0 & 1 \\ 2180 & 0 \end{bmatrix} \quad B = \begin{bmatrix} 0 \\ -14.533 \end{bmatrix} \quad C = [1 \quad 0]$$

Knowing the necessary and sufficient condition to design pole placement controller is reachability and observability of the system, the rank of named matrices are checked. Being full ranked, we proceed with design.

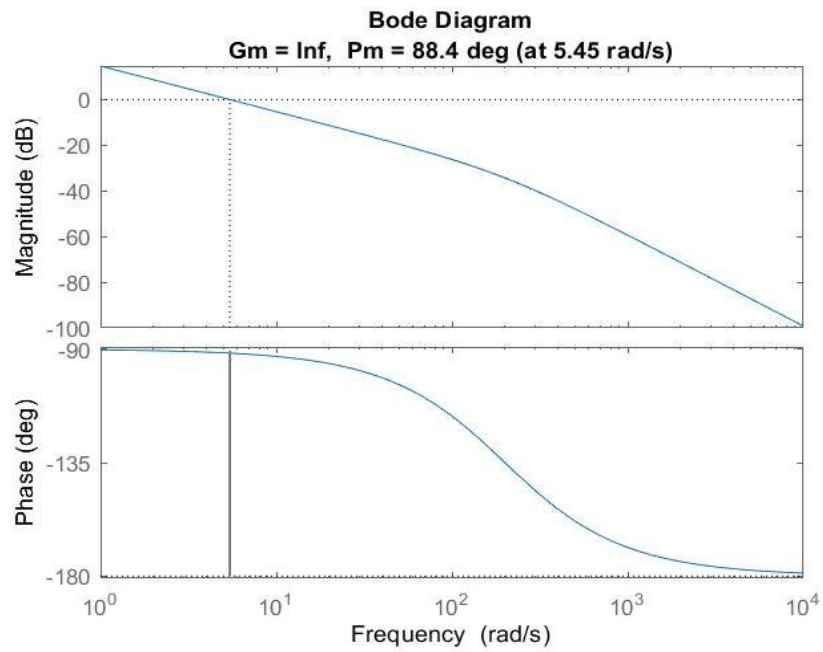
Desired poles: system is of the second order so two poles are required to be specified. Being satisfied with the performance of Root Locus controller, we tried to place the desired poles in a way that the overall performance of the system resembles that of the root locus, furthermore this fact should be considered: the poles need to be chosen such that the outer loop performs at least ten times slower than the inner loop. Hence, the first desired dominant pole is chosen as $P_1 = 20$ and the second pole much faster and far enough as $P_2 = 200$. The method to obtain the state feedback gain is using Ackermann's formula by inserting the inverse of reachability matrix. Finally, state feedback gain: $K = [-425.229 \quad -15.138]$

Another challenge in this project is that there is not any sensor to measure the value of ball speed which it is the second state of the system. To cope with this problem an observer is required to be designed to estimate the amount of ball speed. The observer designed is Luenberger observer. Also, in this case gain of the observer should be designed such that to be much faster than the state feedback so the desired poles considered for the observer would be $P_{o1} = 200$ and $P_{o2} = 201$. And again, to obtain the gain of the observer the Ackermann's formula is used and this time by inserting the inverse of observability matrix. Finally, observer gain: $L = [1001 \quad 252680]'$.

Also, a high-pass filter taking as input the position of the ball is considered as estimator for the speed but the performance was worse so this option has been discarded. At the end an outer loop for zero steady state error is considered and a PI controller is designed in frequency based on the closed loop system of Pole placement. We have also tried to enlarge the system with an integrator but eventually we opted to use the PI because through it we could add a zero, recovering some phase, and so increasing robustness.

$$PI_{pp} = \frac{-1500*(1+0.05s)}{s}$$

This result in an overall cut-off frequency of 5.45 rad/s and 88.4° of phase margin:

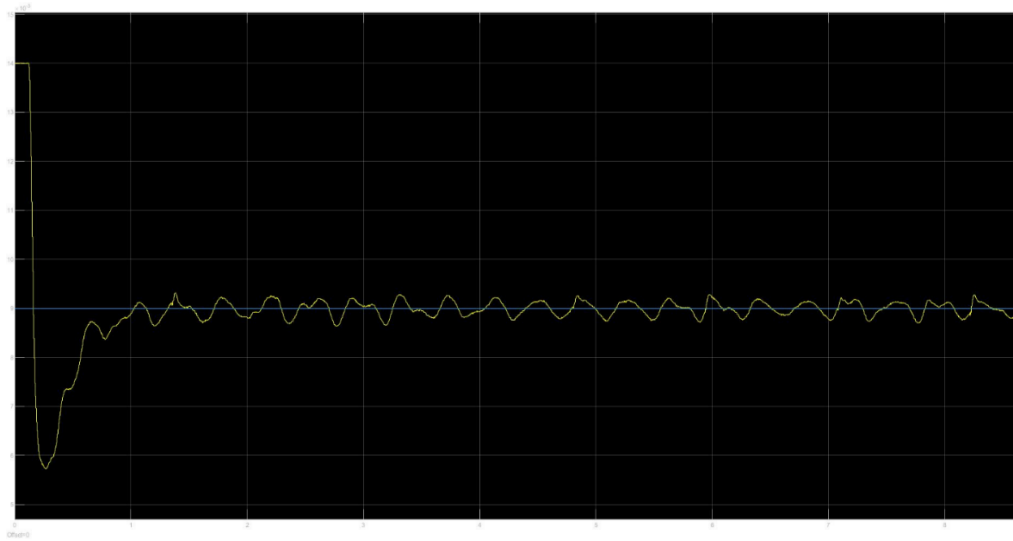


Overall open loop transfer function from reference to position

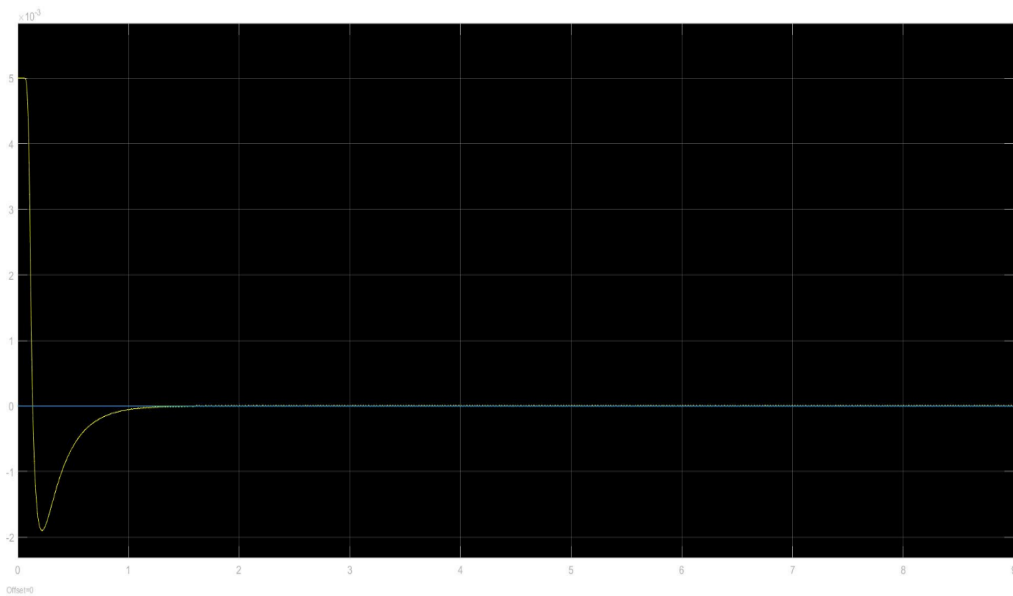
4.2.2.1. Validation of closed loop system with Pole placement position controller in cascade

Here are reported the real and simulated experiments we've performed.

Lift up experiment:

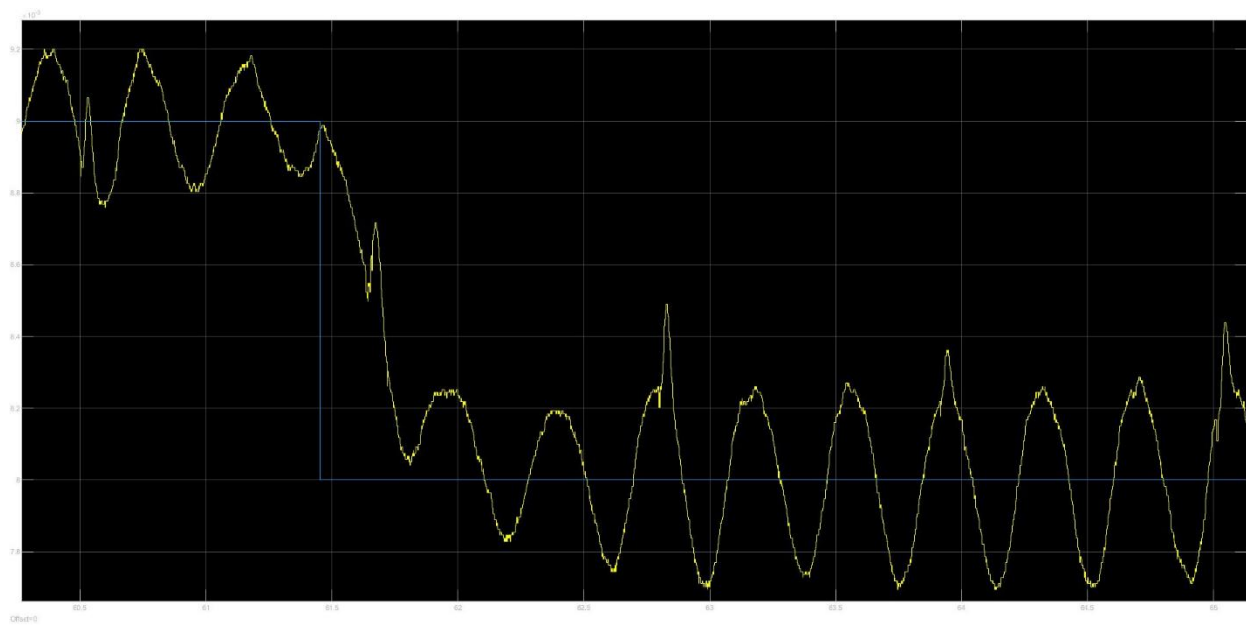


Position scope of the real system during a lift-up from 14 mm to 9 mm

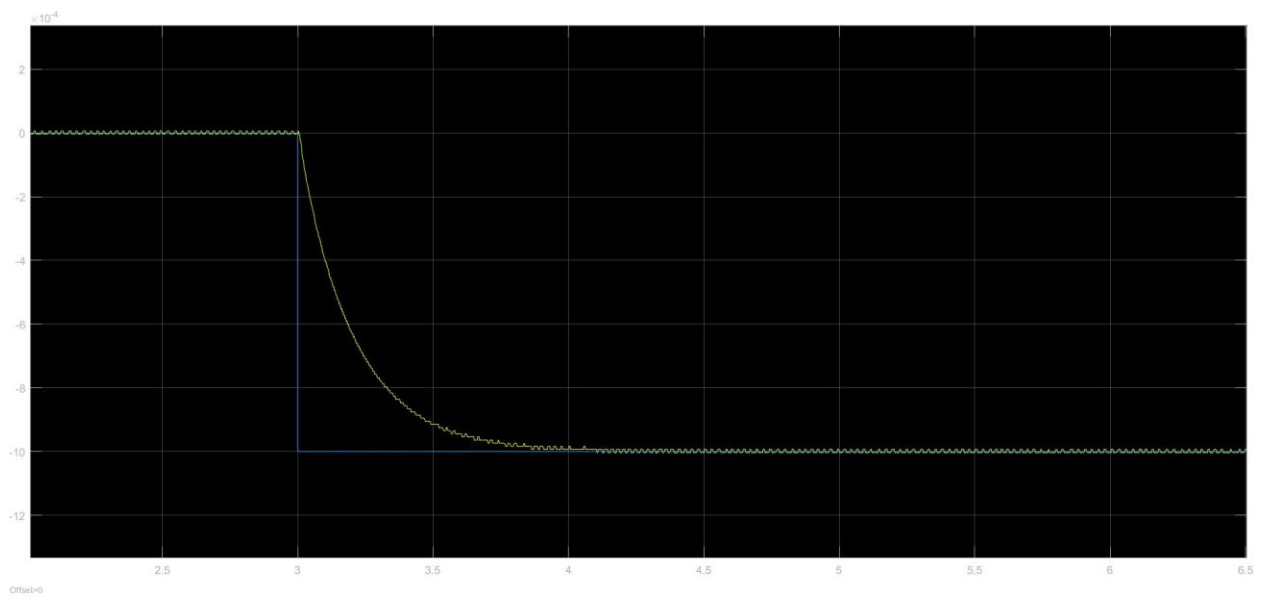


Position scope of the simulated system during the same lift-up

Step response from 9 mm to 8 mm:

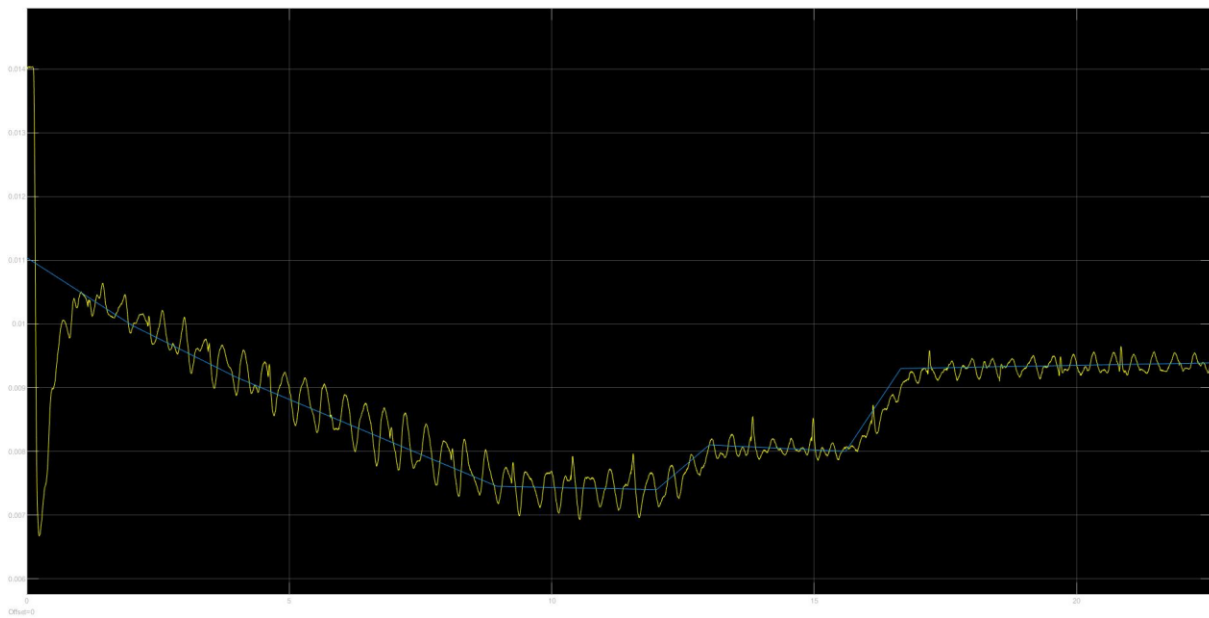


Real system position scope

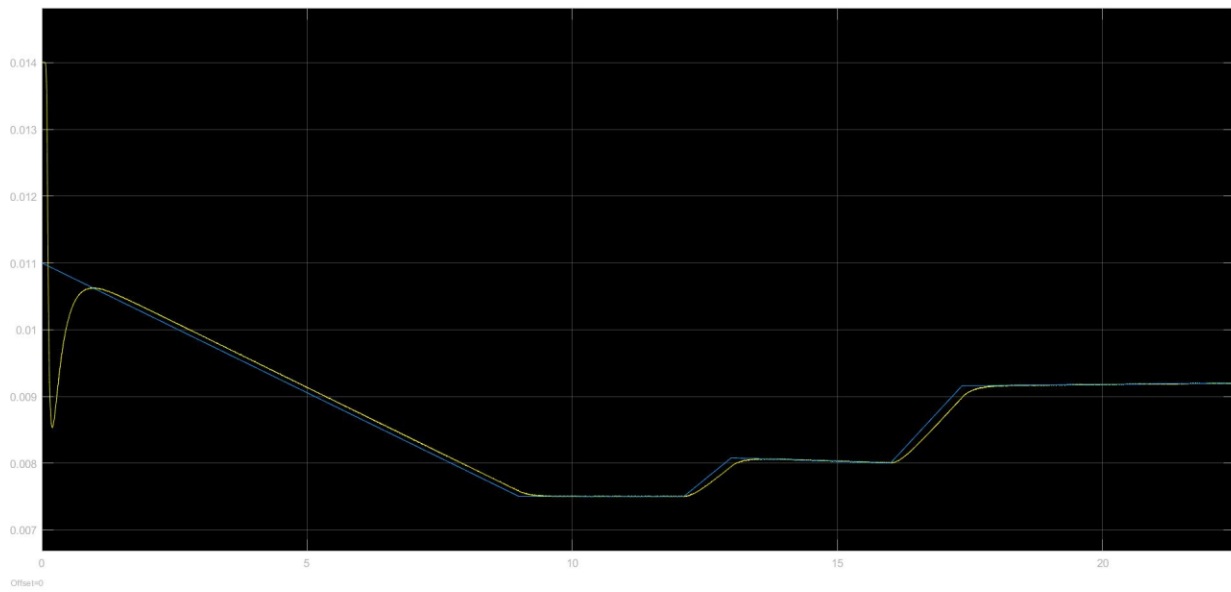


Simulated system position scope

Reference tracking:



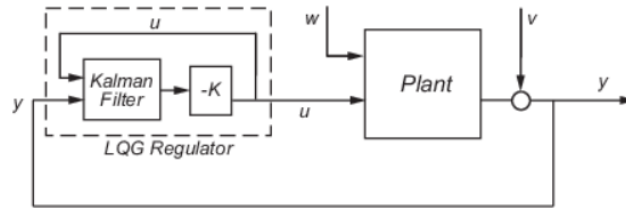
Real system position scope during reference tracking



Simulated system position scope during reference tracking

4.2.3. LQG position controller in cascade

Linear quadratic gaussian control is an optimal controller that provides a control action based on the combination of the solution of the corresponding deterministic LQ control problem and the state estimated by the corresponding Kalman filter. Since our model is nonlinear will use this technique on the linearized system.



$$J = \int_0^T \mathbf{x}^T(t)Q(t)\mathbf{x}(t) + \mathbf{u}^T(t)R(t)\mathbf{u}(t) dt \Big]$$

$I = u(t) = -Kx(t) \quad K = R^{-1} \times B^T \times P \quad \text{Riccati Algebraic equation: } A^T \times P + PA - PBR^{-1}B^TP + Q = 0$

Q is an orthogonal semidefinite positive matrix and represents the weights on the states.

R is an orthogonal positive definite matrix and represents the weights on the control input.

S is a positive definite matrix that penalizes the error from final optimal value.

Therefore, the design parameters are Q and R. We have decided to choose the weights of the position and current (normalized with their respective ranges) in order to obtain a dynamic similar to the one obtained through pole placement. The Kalman Filter have been designed to be much faster than the system dynamics keeping R=1 and playing around with Q to obtain reasonable values.

$$Q_{bar} = 0,01 / D_{bar}^2$$

$$Q = \dot{C} \times Q_{bar} \times C$$

$$R_r = 0,5 / 3^2$$

To obtain the LQR and Kalman gain the function `icare` is used and provide us with these two values.

LQR gain: $K = [-307.233 \quad -6.5023]$

Kalman gain: $L = [551.731 \quad 102203.759]'$

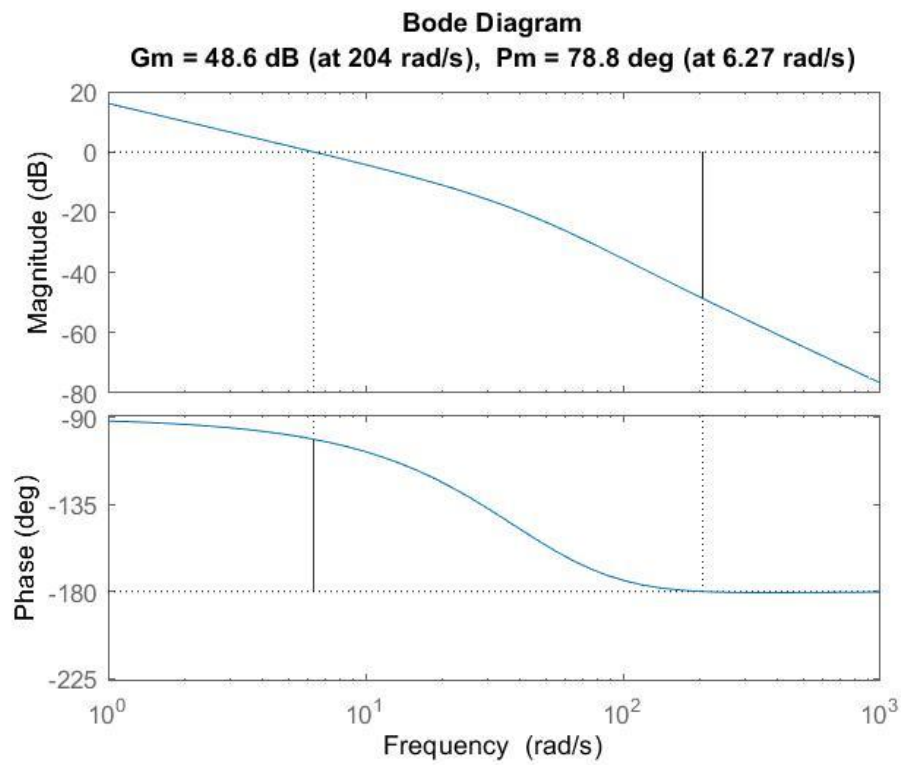
Also, a high-pass filter taking as input the position of the ball is considered as estimator for the speed but the performance was worse so this option has been discarded.

At the end we added an outer loop for zero steady state error designing a PI in frequency based on the closed loop system of LQ.

$$K_{lq} = -1000$$

$$PI_{lq} = K_{lq} \times \frac{1+0.01s}{s}$$

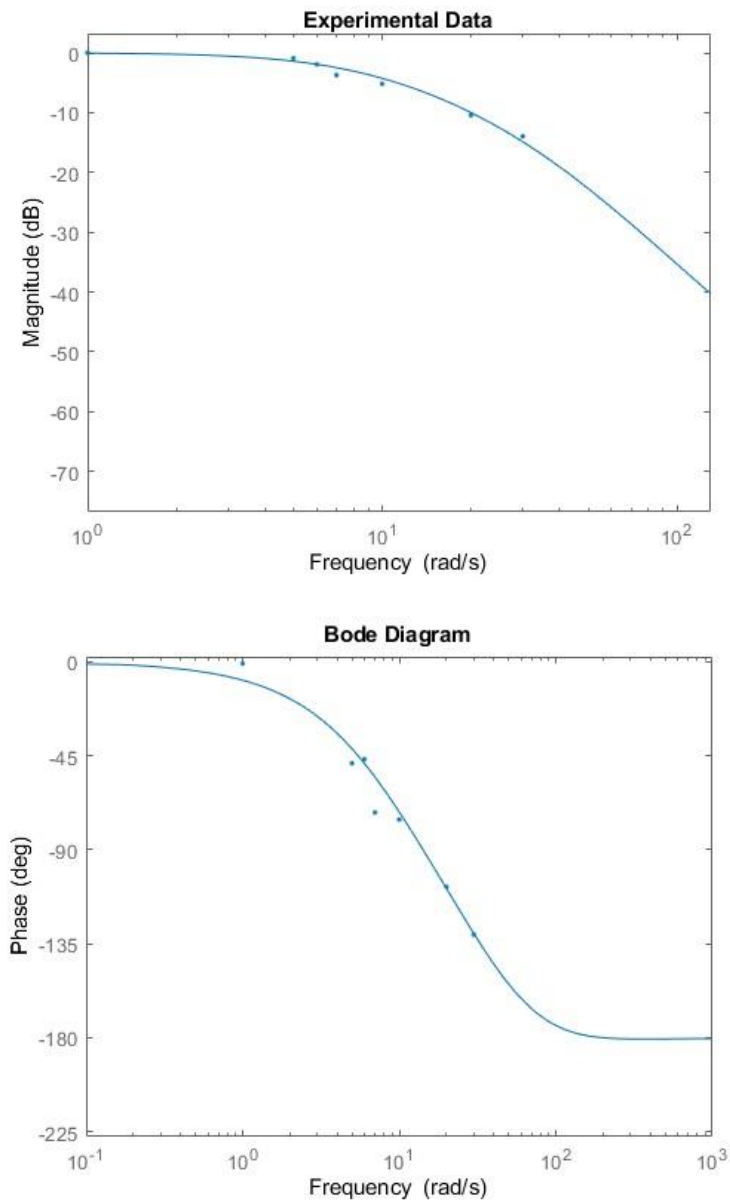
The result in an overall cut-off frequency of 6.27 rad/s and 78.8° of phase margin.



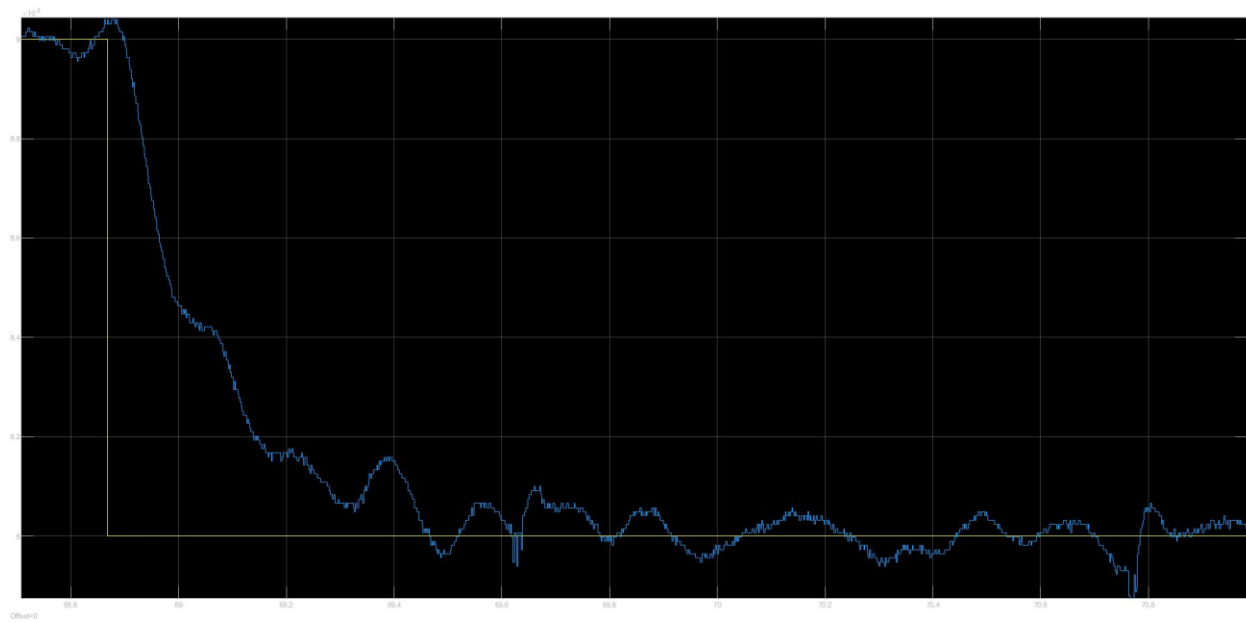
Overall open loop transfer function from reference to position

4.2.3.1. Validation of closed loop system with LQG controller in cascade

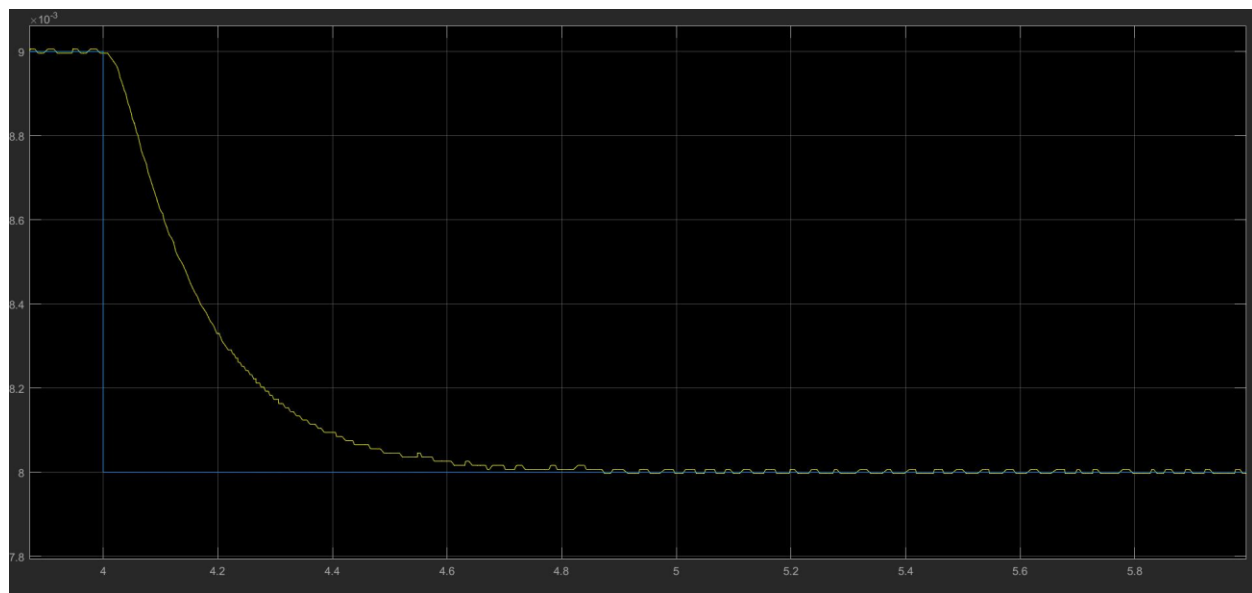
The model has been validated in frequency and time domain. The frequency validation has been made placing the ball in an equilibrium position and applying different sinusoidal waveforms at different ω (taking more points around the dominant pole). The time validation has been made through the system step response.



Step response:



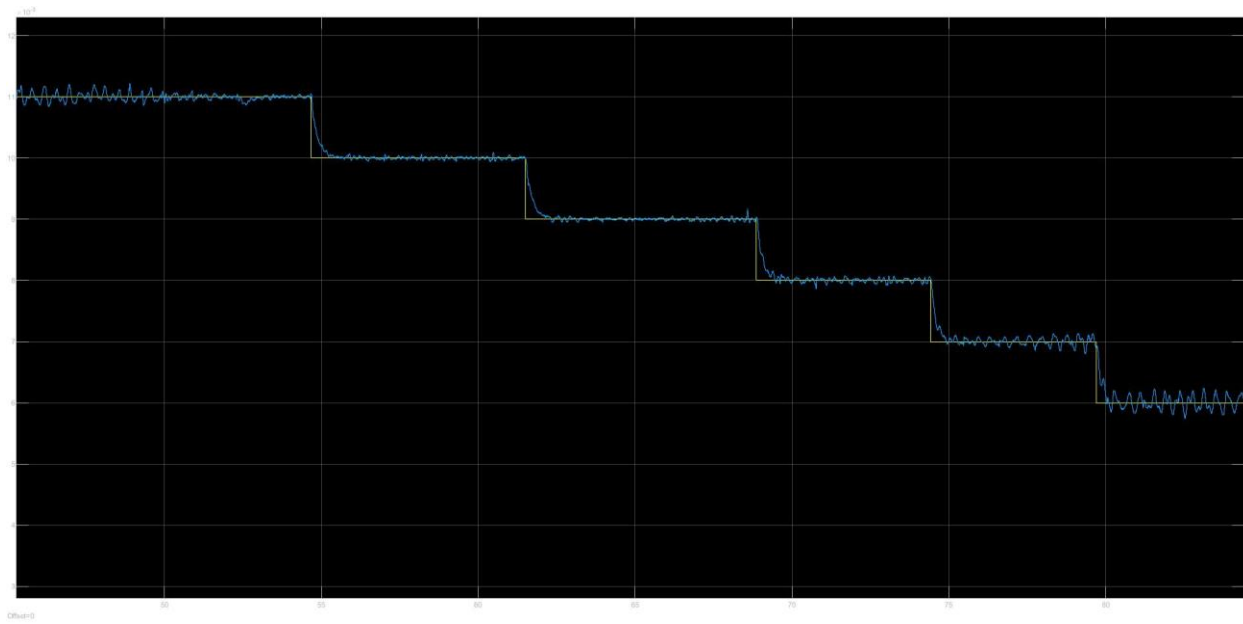
Real system response to a step



Simulated response to a step

Time response $T_r = \frac{5}{\omega} \cong \frac{5}{6.27} = 0.797$

Here increasing steps are applied to show ability to track a reference:



Real system reference tracking

4.2.4. Feedback linearization controller (Advanced)

As last a non-linear control has been designed. Since the parameter K of the magnetic force is not perfectly known and neither constant (it changes with respect to the position) the linearization is fine-tuned directly on the set-up via trial and error. Unfortunately, not much time was left to dedicate to this controller and we think better performances could be achieved with further investigation. Still, this was the only controller we designed able to lift up to 7 mm.

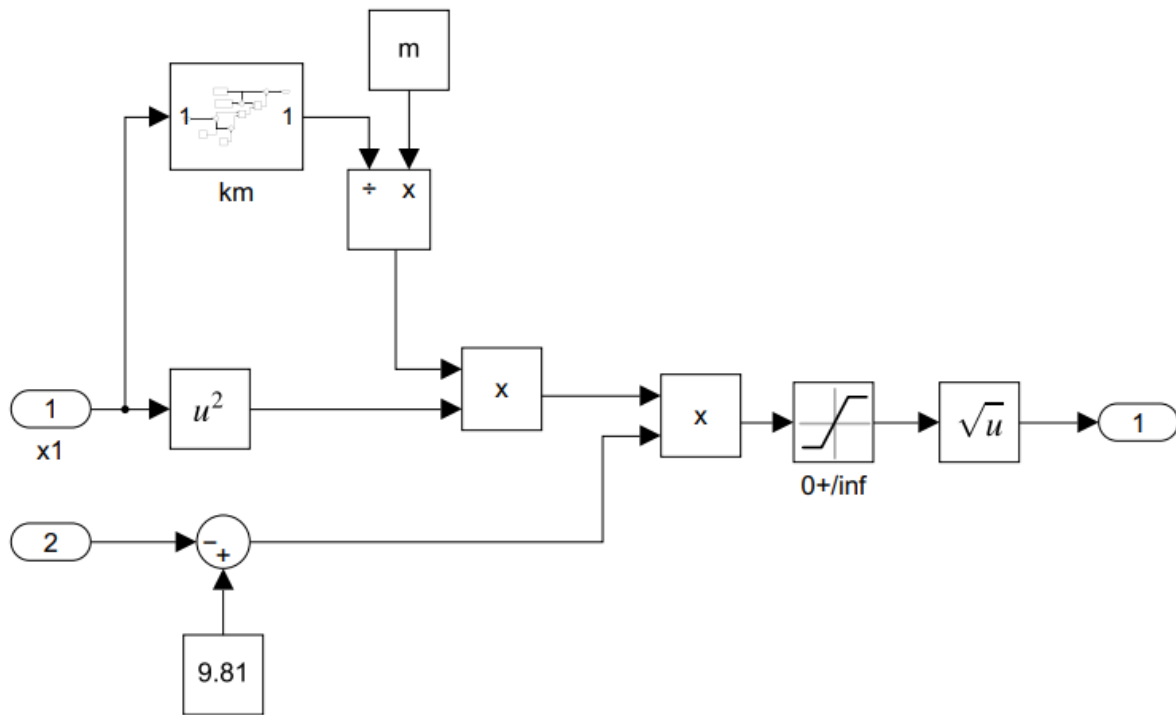
Also, here we kept the inner loop with the PI for current control.

The linearization is performed by simply equating the non-linear part of the system to a signal v .

$$\dot{x}_2 = g - \frac{K i^2}{M x_1^2} = v$$

This procedure leads to a double integrator (being the system of order 2) over which the control has been designed.

$$A_f = \begin{bmatrix} 0 & 1 \\ 0 & 0 \end{bmatrix} \quad B_f = \begin{bmatrix} 0 \\ 1 \end{bmatrix} \quad C_f = [1 \quad 0]$$



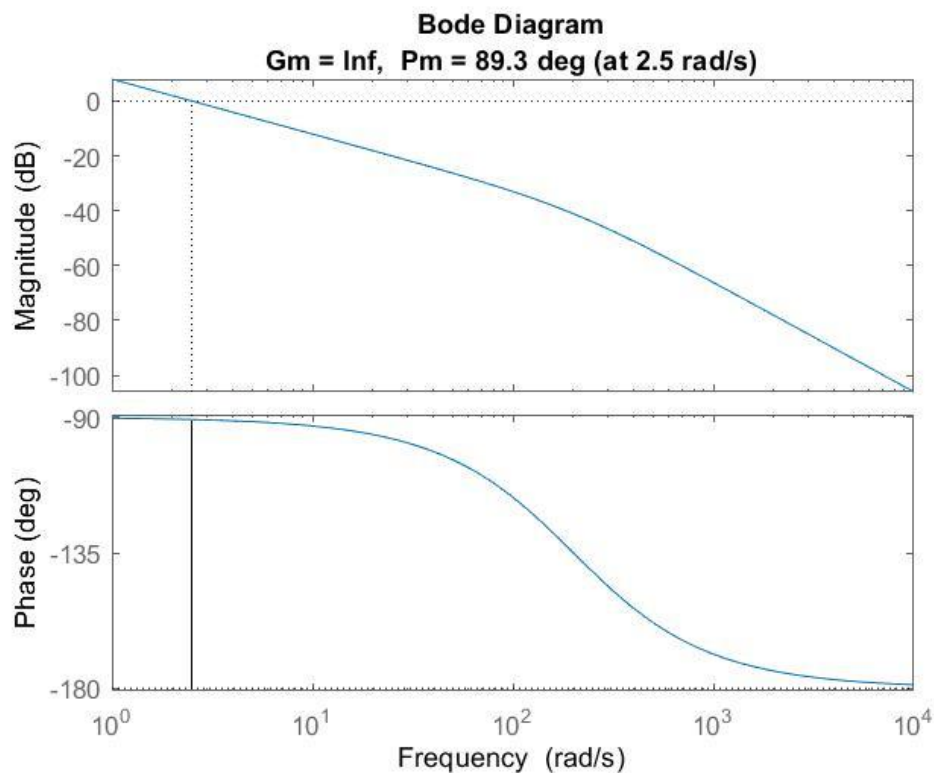
Linearization block

We did not use a constant k but a linear one. With other experiments k could be identified and mapped better. Another problem is that the designed observers were linear, but the system is not: an Extended Kalman Filter could be another way to go.

Other than the part of feedback linearization the design procedure was the same of the PP controller (with the poles placed at $P_1 = 20$ and $P_2 = 200$ and the luenberger observer for speed) with the outer loop PI:

$$PI_{fin} = 10000 \times \frac{1 + 0.05s}{s}$$

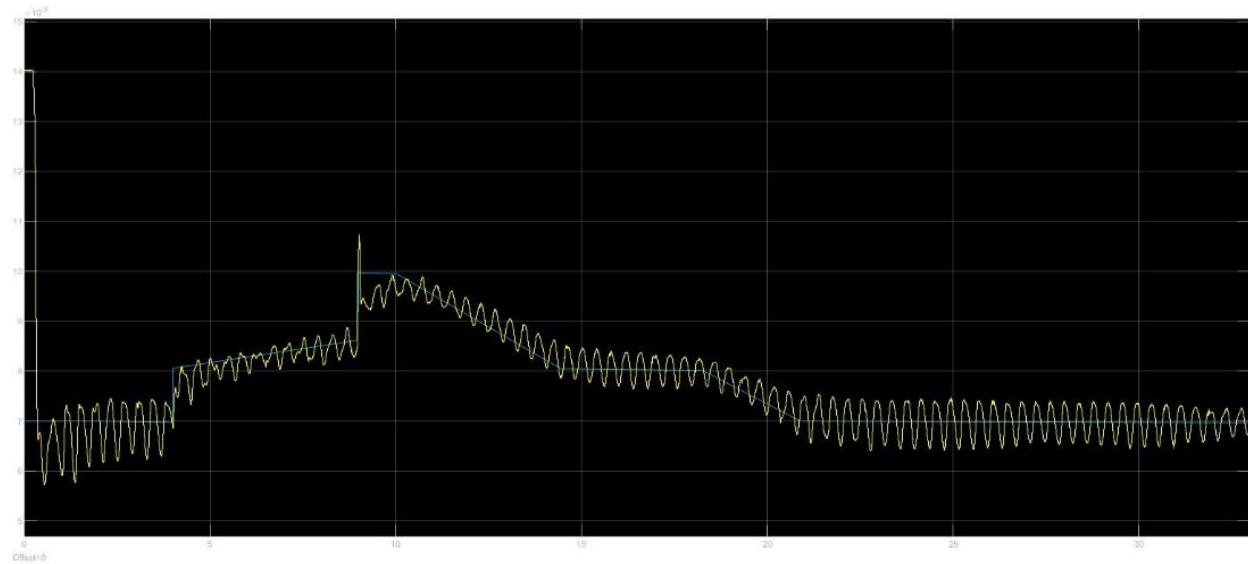
The result in an overall cut-off frequency of 2.5 rad/s and 89.3° of phase margin.



4.2.4.1. Validation of closed loop system with feedback linearization position controller

For the advanced controller just validation in time domain is requested.

Reference tracking and lift up from 14 to 7 mm:



Lift up to 9 mm:

